11th Canadian Masonry Symposium, Toronto, Ontario, May 31- June 3, 2009

BOND BEHAVIOUR OF NSM FRP STRIPS TO MODERN CLAY BRICK MASONRY PRISMS UNDER CYCLIC LOADING

K.M.C.Konthesingha[1a], M.J.Masia[2a], R.B.Petersen[3a], A.W.Page[4a]

[1] PhD candidate, Chaminda.Konthesinghamuhandiramlage@studentmail.newcastle.edu.au, [2] Senior Lecturer, Mark.Masia@newcastle.edu.au , [3] PhD candidate, robert.petersen@studentmail.newcastle.edu.au, [4] Emeritus Professor, Adrian.Page@newcastle.edu.au

[a] Centre for Infrastructure Performance and Reliability, School of Engineering, The University of Newcastle, University Drive, Callaghan, NSW 2308, Australia.

ABSTRACT

The results of pull tests performed on six near surface mounted (NSM) CFRP retrofitted clay brick masonry prisms are presented in this paper. Quasi static cyclic axial displacements were applied to the FRP strip (inducing shear in the bond between strip and masonry). The specimens were subjected to increasing cycles of displacement until failure occurred. Two loading histories were used for the experiment. The results presented here include the bond strength, critical bond length and cyclic bond slip behaviour. The degradation due to cyclic loading compared to monotonic loading is also discussed using the results of similar specimens tested for monotonic loading.

KEYWORDS: Masonry, Retrofit, Fibre reinforced polymer, Slip, Bond, Cyclic loads

INTRODUCTION

Unreinforced masonry (URM) buildings are highly prone to damage during an earthquake [1, 2]. Many existing buildings were designed and constructed before the development of rational earthquake design procedures [3]. For example, in Australia, buildings were not designed to withstand earthquake loads until after the Newcastle earthquake in 1989 [4]. There is a strong need to introduce cost effective seismic retrofitting methods for URM buildings. Furthermore, to protect the appearance of such buildings, many having heritage significance, the methods should have a low aesthetic impact.

There are many conventional seismic retrofitting techniques for URM walls. These techniques include surface treatment with ferrocement or shotcrete, grout injection, external reinforcement with steel and joint repointing. The advantages and disadvantages of these techniques have been discussed by others [5, 6]. The main disadvantages are that they may: add considerable mass, reduce space, require skilled labour, interrupt the normal function of the building, be costly and restrict the use of certain types of buildings [1, 6, 7].

Fibre reinforced polymer (FRP) strengthening is emerging as an effective seismic retrofitting technique for URM buildings. The FRP strengthening method has several advantages compared with conventional retrofitting techniques. FRP materials have a high strength and stiffness to weight ratio and high durability. Also, there is a minimal loss of usable space due to the strengthening application and it is relatively easy to install [1, 2, 8, 9, 10]. In addition to the above advantages, FRP reinforcement will also resist crack propagation [2].

There are three common types of FRP namely Glass (GFRP), Aramid (AFRP) and Carbon (CFRP) [11]. FRP is manufactured in different shapes such as rods, sheets, tendons, laminates and strips. Two techniques are used to bond the FRP reinforcement to masonry walls; (i) FRP sheets, laminates or strips can be externally bonded (EB) to the surface of a wall; (ii) FRP strips or rods can be inserted into grooves cut into the surface of a wall using a technique known as near surface mounting (NSM). Of these two techniques, the NSM technique provides several advantages; higher strain can develop in the FRP before debonding, the FRP is protected from vandalism and to some extent from fire and other environmental influences, and the technique has a minimal impact on the aesthetics of the structure [12]. Thin rectangular FRP strips inserted with their greater dimension normal to the surface of the wall are considered to be the most efficient reinforcement cross section shape for the NSM technique [12].

FRP retrofitting/strengthening schemes may fail by FRP rupture or, more commonly, by debonding either at the FRP masonry interface (epoxy failure) or within the masonry itself. Therefore, understanding the bond behaviour between masonry and FRP is essential to assessing the effectiveness of the retrofitting scheme. The experimental pull test [12] may be used to study the bond behaviour between masonry and FRP reinforcement. Several pull test experiments were previously conducted by researchers to identify the bond behaviours between masonry and NSM FRP [12, 13]. In these tests monotonic load was applied until failure occurred. To evaluate the effectiveness of the retrofitting technique under seismic loading it is also important to quantify the bond slip behaviour under cyclic loading. Although quasi static cyclic loading for in plane and out of plane tests have been conducted on FRP strengthened walls [2, 9, 10, 14, 15], the authors were unable to find any published literature focusing on the cyclic bond behaviour between FRP and brick masonry. There are, however, some researchers who performed experiments to investigate the bond behaviour between FRP and concrete under cyclic loading. [16] used beam pull tests to investigate the bond behaviour between NSM CFRP and concrete under cyclic and monotonic loading. They found that the peak pull out force was not influenced by the cyclic loading. Also, [17] have derived local bond stress-slip relationships for FRP bonded to concrete by testing 54 pull test specimens under monotonic and cyclic loading conditions.

The current paper presents the results of six pull tests performed to investigate the bond behaviour between NSM FRP and masonry under quasi static cyclic loading. The bond strength, critical bond length and local bond slip relationship under cyclic loading was determined. The degradation due to cyclic loading compared to monotonic is also discussed by comparing the results to those of similar specimens tested for monotonic loading.

EXPERIMENTAL PROGRAM

Six identical pull test specimens were tested. Each specimen consists of a four brick high stack bonded prism (Figure 1) constructed using solid clay bricks with the nominal dimensions of

230mm x 110mm x 76mm (length x width x height). The flexural tensile strength of the bricks was determined from lateral modulus of rupture tests [18]. The mortar used to construct the specimens was mixed in a ratio of 1:1:6 (cement: lime: sand by volume). The flexural tensile strength of the mortar joint was determined using the bond wrench test [19]. Two 1.4 mm thick by 15 mm wide carbon FRP strips were glued together with an Araldite^{TM} epoxy adhesive to make 2.8 mm thick by 15 mm wide carbon FRP strips. The purpose of gluing two strips together was to achieve a ratio of FRP cross sectional area to bonded perimeter which ensured that debonding failure occurred instead of FRP strip rupture. After preparation of each masonry prism, a groove was cut into the surface using a brick cutting saw and the FRP strip was glued into groove with a two-part epoxy adhesive. The elastic modulus of the FRP strip was determined for each specimen during the pull tests from two strain gauges, placed on either side of the unbonded portion of the strip (strain gauges 9 and 10 in Figure 1b). The material properties are shown in Table 1.

Table 1: Material properties

Material	Property	Mean	Standard deviation	Source
Masonry units	Lateral modulus of rupture (MPa)	3.57	0.75	Petersen et al. [12] (average of 4 specimens)
Mortar batch	Flexural tensile strength (MPa)	0.52	0.21	AS3700 – 2001 [19] (average of 10 joints)
CFRP	Elastic modulus (MPa)	207050	7643.62	Current pull test (average of 6 specimens)
CFRP	Rupture Strain (με)	12000	-	Manufacturers data
Epoxy	Flexural strength (MPa)	>30	-	Manufacturers data

In four of the specimens, strain gauges were also installed to record the strain distribution along the bonded length of the FRP (Figure 1a). The gauges were inserted between the two FRP strips before they were glued together so that they would not influence the bond between the FRP strip and the masonry.

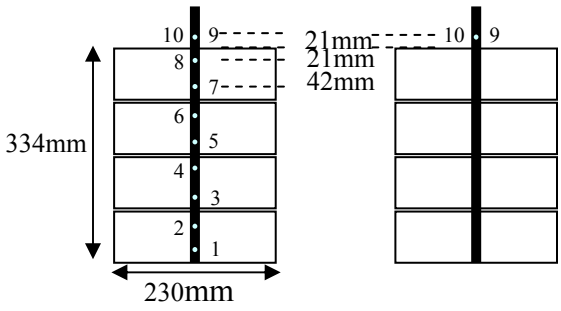

(a) **(b)**

Figure 1: Pull test specimens showing strain gauge locations for (a) Specimens 1A, 1B, 2A and 2B (b) Specimens 1C and 2C

Figure 2 shows the test setup. The base plate of the apparatus was first attached to the bottom of an Instron Universal Testing Machine. This machine was used to apply the quasi static cyclic displacement to the FRP strip. The specimen was then positioned on top of the base plate. A 5mm thick plywood sheet and a 12mm thick steel specimen plate were placed on top of the

specimen. Finally, the top restraining plate was tied down and horizontally levelled using bolts. Both the specimen plate and plywood had a small slot cut into the edge to allow the FRP strip to pass through. The plywood was used to ensure full contact between the top of the masonry specimen and the 12 mm specimen plate.

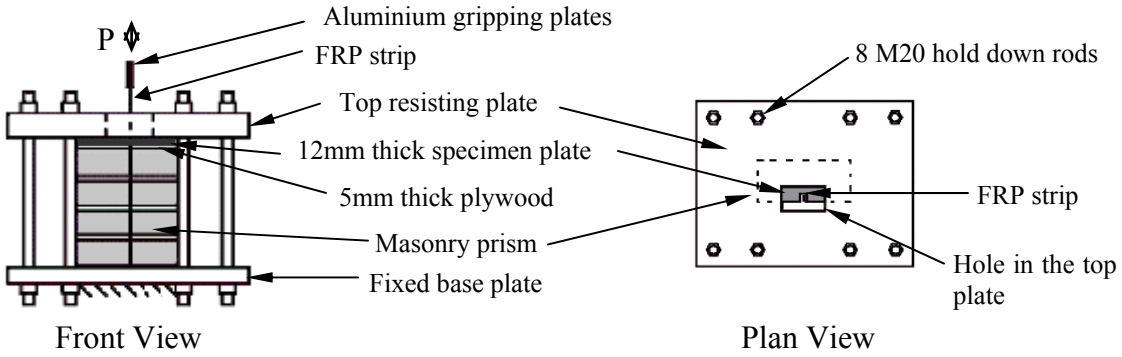

Figure 2: Experimental test setup

To determine the displacement history to be used for the pull tests consideration was given to the conditions likely to be present in a retrofitted masonry wall subjected to cyclic in-plane shearing. As a shear wall is displaced laterally in-plane, FRP reinforcement strips in the tension region will be subjected to tensile strain. Depending on the magnitude of the applied displacement, the wall may crack and the FRP may partially debond. When the displacement direction reverses, the FRP strip will unload and as the wall returns to its starting position, any cracks will close and the FRP will have completely unloaded. If some FRP debonding has occurred then the FRP may be subjected to some compression in returning to its starting position. As the wall travels past its starting position and displaces in the other direction the FRP reinforcement which was subjected to tensile strain in the first half displacement cycle may now be located in a compression region of the wall. In this instance the compressive loads will be shared by the masonry and FRP in proportion to their relative areas and stiffnesses and the shear stress transferred between the masonry and FRP will be negligible. This behaviour will then repeat with each full cycle of displacement until failure occurs.

The current pull tests were designed to simulate such behaviour. Therefore, a displacement history in which the FRP is subjected to cycles of tensile displacement which is returned to zero displacement after each cycle was considered to be the most representative of the behaviour in a retrofitted wall. Prior to testing it was expected that returning the FRP displacement to zero after each cycle would induce some compressive force into the FRP strips but it was not known whether the compression would be sufficient to cause buckling of the FRP over its free length. Therefore, an alternative displacement/load history was also trialled. The latter used the same cyclic displacement history as the former but after each cycle the tensile load (rather than tensile displacement) was returned to zero. In this way, the risk of buckling of the FRP was removed, offering a more robust test approach for future use if the two approaches were observed to yield similar overall results.

The adopted quasi static cyclic displacement histories are shown in Figure 3 and were determined in accordance with the recommendations of [20]. The vertical axes in Figure 3 represent the displacement of the universal testing machine grips attached to the free end of the

FRP strip. The displacement increments of 1.5 mm, each applied for three full cycles, were selected such that each increment represented approximately 10-15% of the displacement required to reach maximum load in a monotonic pull test as reported in [12]. The specimens were subjected to increasing cycles of displacement until failure occurred. After each cycle of displacement, the load was returned to zero for Load case 1 and the displacement was returned to zero for Load case 2. For each loading pattern, three specimens were tested. Two out of the three samples included strain gauges along the bonded length (Figure 1a).

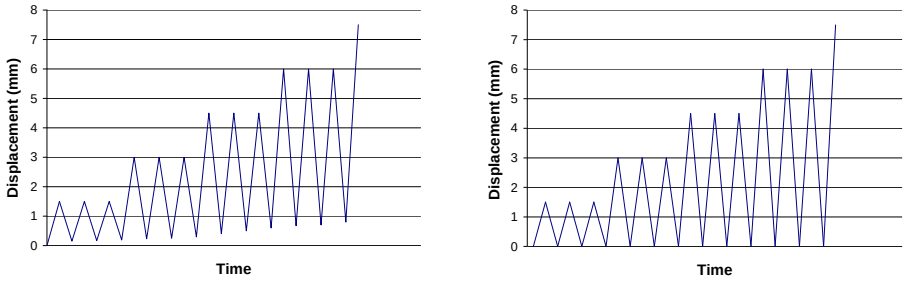

(a) **(b)**

Figure 3: Time history (a) load case 1 (b) load case 2

EXPERIMENTAL RESULTS

The experimental results are summarised in Table 2. Four out of six specimens failed by debonding within the masonry material (Figure 4a). Cracks first appeared close to the loaded end and then extended further down the specimen with increasing displacement until the FRP strips completely debonded. After removing the specimens from the apparatus, cracks were observed extending through the thickness of the specimen, in line with the FRP (Figures 4b and 4c). This type of cracking most likely resulted from lateral tensile stresses induced in the prisms by shear induced dilation upon FRP debonding. This was common to all four specimens which debonded through the brick. The other two specimens failed by debonding/sliding along the interface between the FRP and epoxy (Figure 4d).

(a) **(b)** **(c)** **(d)**

Figure 4: Typical failure modes (a) Debonding failure (b) Cracks in the back face of the specimen (c) Cracks at the top of specimen (d) Adhesive failure

The pull test was used to identify three parameters, namely bond strength, critical bond length and cyclic bond slip behaviour of masonry retrofitted with FRP strips under cyclic loading. For specimens 1A, 1B, 2A and 2B with strain gauges distributed along the FRP bonded length, the local slip of FRP relative to masonry was calculated by numerically integrating the strain

distributions at increasing load increments up to the failure load. Two assumptions were made for calculating the slip; the axial strain in the masonry is negligible and the slip at the unloaded end is zero. Load versus displacement (relative slip between the FRP and masonry at the loaded end of the specimen) for Specimen 1A is shown in Figure 5a. The plot shows that the stiffness reduced with increasing displacement cycles. Figure 5b shows the comparison of the load-displacement relationships for the two loading cases. It can be seen that the stiffness reduced more rapidly with displacement cycles for Load case 2 than Load case 1 but in general the load-displacement behaviour is almost the same for both load cases. Furthermore, the compression load required to return the FRP strip displacement to zero in Load case 2 was observed to be negligible making the observed responses under the two load cases very similar.

Table 2: Summary of experimental results

Loading pattern	Specimen ID	Load on first Crack (kN)	Failure load (kN)	Maximum load (kN)	Failure mode	Displacement cycle observation	
						First crack	Failure
Load case 1	1A	48	50	61.5	Debonding (Masonry failure)	1st cycle of 6mm displacement	3rd cycle of 9mm displacement
	1B	35	56.8	56.8	Pull out (Adhesive failure)	1st cycle of 6mm displacement	1st cycle of 9mm displacement
	1C	46	58	58	Pull out (Adhesive failure)	1st cycle of 6mm displacement	1st cycle of 7.5mm displacement
Load case 2	2A	30.5	63	64	Debonding (Masonry failure)	1st cycle of 4.5mm displacement	1st cycle of 9mm displacement
	2B	33	58	63	Debonding (Masonry failure)	3rd cycle of 7.5mm displacement	1st cycle of 10.5mm displacement
	2C	45	66.5	66.5	Debonding (Masonry failure)	1st cycle of 6mm displacement	1st cycle of 9mm displacement

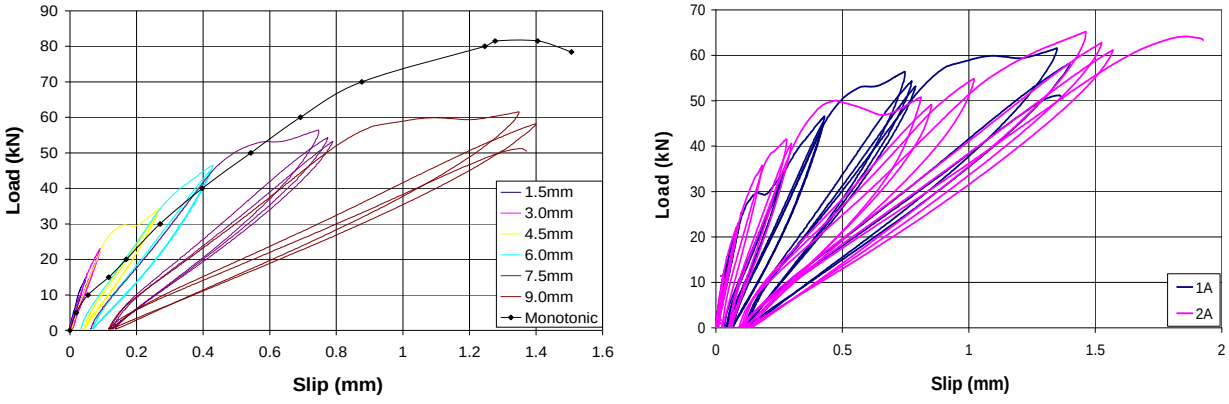

(a) **(b)**

Figure 5: (a) Load displacement curve for Specimen 1A (b) Comparison of load displacement curves for Specimens 1A and 2A

Petersen et al. [12] conducted a similar study for nominally identical specimens under monotonic loading. The results obtained by Petersen et al. [12] were used here to investigate the degradation due to cyclic loading compared to monotonic loading. The load-displacement curve, bilinear bond slip curve and the bond strength for pull tests under monotonic loading are shown in Figure 5a, Figure 7b and Table 3 respectively [12].

The shear stress transferred from the FRP to the masonry through the epoxy was determined from the strain distributions, for all specimens with strain gauges using the following equation.

$$\tau_{avg} = \frac{(\Delta\varepsilon)E_p b_p t_p}{(\Delta L)(2b_p + t_p)} \tag{1}$$

Where τ_{avg} = average shear stress transferred from the FRP to the masonry through the epoxy over the length ΔL; $\Delta\varepsilon$ = change in strain over length ΔL; E_P = Elastic modulus of FRP strip; b_p = width of strip; t_p = thickness of strip; and ΔL = incremental length along FRP (equal to strain gauge spacing).

Figure 6 shows the shear stress distribution along the FRP strip for Specimen 2B. The critical bond length is the bonded length required to develop full bond strength. The critical bond length was estimated from the shear stress distribution (at the maximum load) as the distance between the 2 points: i) where interface cracks are fully developed and the shear stress is approximately equal to zero; and ii) in the uncracked masonry where the shear stress is approximately equal to zero. For specimen 2B in Figure 6, these points were determined from the curve plotted at 63.5 kN as: 50 mm (i) and 250 mm (ii). The critical bond length was then 200 mm. For all specimens the average critical bond length was found to be 225mm.

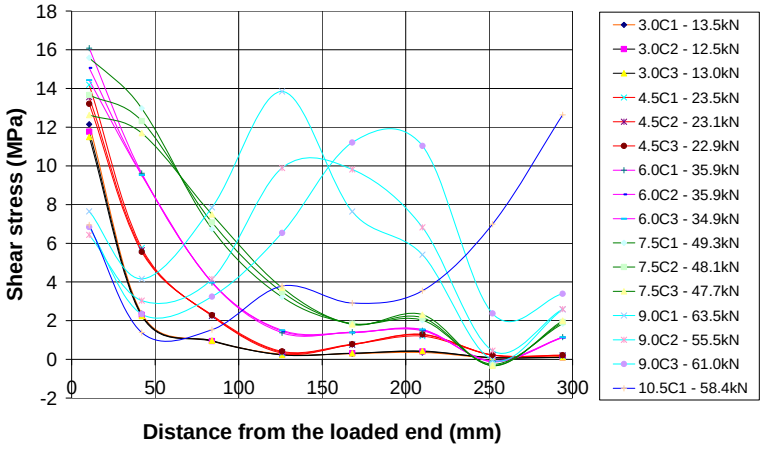

Figure 6: Shear stress versus distance from loaded end for Specimen 2B

Next, the relative slips and the shear stresses along the bonded length for all imposed displacements were calculated for each specimen. This allowed bond (shear stress) versus slip (shear displacement) to be plotted as shown in Figure 7a for Specimen 1A. Single idealized bilinear bond slip models were derived for each specimen for use in finite element modelling and

for analytical modelling. The maximum shear stress (τ_{max}) and corresponding slip (δ_1) were averaged from the experimental bond slip curves. The bond slip curve 10.5mm from the loaded end was ignored when calculating maximum shear stresses because it was affected by the restraint conditions at the loaded end. A back calculation of Equation 2 using the experimentally determined bond strength for P_{IC} was used to determine the final slip (δ_{max}) (as done in [12]). It was found that, for each sample the bilinear bond slip models developed here reasonably fit with the experimental bond slip data. The bilinear model for sample 1A is shown in Figure 7a.

$$P_{IC} = \sqrt{\tau_{\max}\delta_{\max}}\sqrt{L_{per}(EA)_P} \qquad (2)$$

Where P_{IC} = the bond strength of the specimen, L_{per} = bonded perimeter of FRP which was 32.8 mm, $(EA)_P$ = axial stiffness of the strip.

The bilinear bond-slip curves for specimens 1A, 2A and 2B and are shown in Figure 7b. Due to the sliding failure of sample 1B, a bilinear bond slip curve could not be determined from the test data.

As shown in Figure 7a, during some parts of the applied displacement history, negative shear stresses are observed even for Load Case 1 in which the load applied to the FRP is at all times tensile. Negative shear stress implies that the axial strain in the FRP is increasing (rather than decreasing) with distance from the loaded end of the specimen (Equation 1). This is believed to result from the discrete locations of some strain gauges coinciding with a debonding crack in the specimen and therefore recording a higher strain than an adjacent gauge, closer to the loaded end, at which the FRP is sharing the tensile load with well bonded surrounding masonry. This phenomenon disappears with distance from the loaded end and for higher applied displacements/loads.

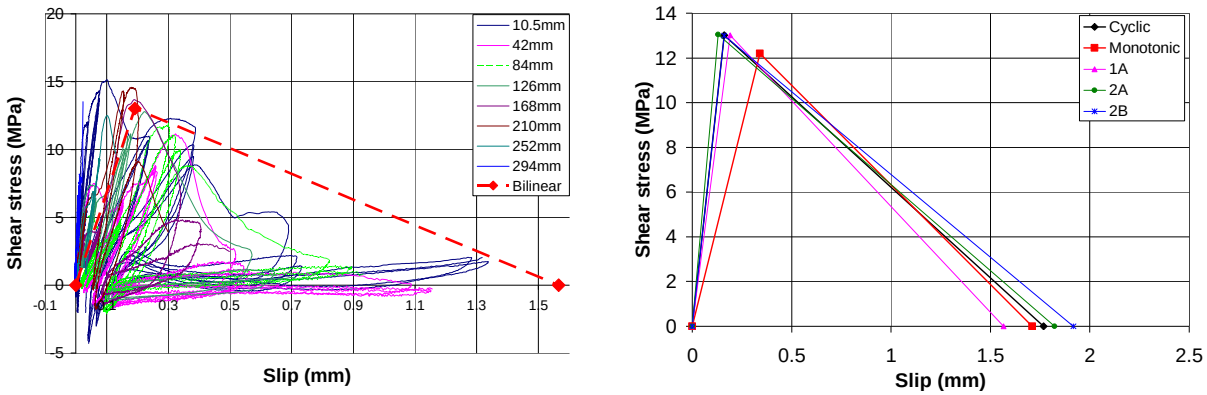

(a) **(b)**

Figure 7: (a) Bond slip curve for Specimen 1A (b) Bilinear Bond behaviour under cyclic and monotonic loading

Comparing the results in Table 3, the average failure load for Load case 2 was unexpectedly found to be approximately 13% higher than Load case 1. This can possibly be attributed to the two adhesive failures in Load case 1 (Specimens 1B and 1C) dragging down the mean failure load. Figure 5a shows the load displacement curves for cyclic and monotonic loading. Table 3

shows the bond strength comparison between monotonic and cyclic loading patterns. It can be seen that generally there is approximately 20% reduction in the bond strength for cyclic loading compared with monotonic. Figure 7b shows that the monotonic and cyclic bilinear bond slip curves show very similar relationships independent of the loading pattern. However, to confirm this observation, further experiments with more test specimens are needed. If this observation can be confirmed then considerable efficiency will result as numerical modelling of cyclic behaviour could be based on monotonic, rather than cyclic, pull tests. The former are considerably easier to conduct.

Table 3: Results comparison

Loading pattern	Average Bond Strength (kN)	
	Load case 1	Load case 2
Quasi static cyclic	58.77	64.5
Monotonic	78.67	
Percentage degradation %	**25.3**	**18.01**

CONCLUSION

Six pull test specimens were tested to identify the local bond slip behaviour between FRP and clay brick masonry under cyclic loading. The NSM technique was used and two cyclic load cases were applied. It was found that the reduction in the bond strength under cyclic loading compared with monotonic loading is around 20%. The stiffness was reduced in load case 2 compared to load case 1. Although a 13% increase in the average bond strength was observed for load case 2 compared to load case 1, more tests are required to better quantify the relationship between load cases 1 and 2. Bond slip behaviours of the two loading cases are very similar. Also bond slip curves for monotonic and cyclic loading cases were approximately similar. If this observation can be verified with further testing then it may be possible to numerically model cyclic debonding behaviour using bond slip curves established from monotonic tests.

ACKNOWLEDGEMENTS

The authors gratefully acknowledge the support of the technical staff of the Civil, Surveying and Environmental Engineering Laboratory at The University of Newcastle. The support given by undergraduate student K.C. Chin is appreciated very much. The financial support for this project was provided by the Australian Research Council under Discovery Project DP 0879592.

REFERENCES

1. El-Dakhakhni, W. W., Hamid, A. A., Hakam, Z. H. R., and Elgaaly, M. (2006) “Hazard mitigation and strengthening of unreinforced masonry walls using composites” Composite Structures, 73(4), 458-477.
2. ElGawady, M. A., Lestuzzi, P., and Badoux, M. (2006) “Shear strength of URM walls retrofitted using FRP” Engineering Structures, 28(12), 1658-1670.
3. Shrive, N. G. (2006) “The use of fibre reinforced polymers to improve seismic resistance of masonry” Construction and Building Materials, 20(4), 269-277.
4. Page, A. W. (1996) “Earthquake and unreinforced masonry structures - An Australian overview” Research Report No.136.4.1996, Department of Civil Engineering and Surveying, University of Newcastle, NSW, Australia.

5. Corradi, M., Borri, A., and Vignoli, A. (2008) "Experimental evaluation of in-plane shear behaviour of masonry walls retrofitted using conventional and innovative methods" The Journal of the British Masonry Society, Masonry International, 21(1), 29-42.
6. ElGawady, M., Lestuzzi, P., and Badoux, M. (2004) "A review of conventional seismic retrofitting techniques for URM" 13th International Brick and Block Masonry Conference, Amsterdam.
7. El-Dakhakhni, W. W., Hamid, A. A., and Elgaaly, M. (2004) "In-plane strengthening of URM infill wall assemblages using GFRP laminates" The Masonry Society Journal, 22(1), 39-50.
8. Silva, P. F., Belaebi, A., and Li, T. (2006) "In-plane performance assessment of URM walls retrofitted with FRP" The Masonry Society Journal, 24(1), 57-68.
9. Korany, Y., and Drysdale, R. (2004) "Enhancing seismic flexural resistance of historic masonry walls using Carbon Fiber Rope" The Masonry Society Journal, 22(1), 27-38.
10. Zhoa, T., Zhang, C., and Xie, J. (2004) "Shear behaviour of UCMW using CFRP sheet: A case study" The Masonry Society Journal, 22(1), 87-95.
11. Zhuge, Y. (2008) "FRP retrofitted URM walls under in-plane shear - A review of available design models" 14th International Brick and Block Masonry Conference, Sydney, Australia, on CD-ROM.
12. Petersen, R. B., Masia, M. J., and Seracino, R. (2008) "Bond Behaviour of NSM FRP Strips Bonded to Modern Clay Brick Masonry Prisms: Influence of Strip Orientation and Compression Perpendicular to the Strip" Journal of Composites for Construction, (in press).
13. Willis, C. R., Yang, Q., Seracino, R., and Griffith, M. C. (2008) "Bond behaviour of FRP-to-clay brick masonry joints" Engineering Structures, (revised manuscript submitted 04/08)
14. Ghobarah, A., and Galal, K. E. M. (2004) "Out-of-Plane Strengthening of Unreinforced Masonry Walls with Openings" Journal of Composites for Construction, ASCE, 8(4), 298-305.
15. Ehsani, M. R., Saadatmanesh, H., and Velazquez-Dimas, J. I. (1999) "Behaviour of retrofitted URM walls under simulated earthquake loading" Journal of Composites for Construction, ASCE, 3(3), 134-142.
16. Cruz, J. M. S., Barros, J. A. O., Gettu, R., and Azevedo, A. F. M. (2006) "Bond Behavior of Near-Surface Mounted CFRP Laminate Strips under Monotonic and Cyclic Loading" Journal of Composites for Construction, ASCE, 10(4), 295-303.
17. Ko, H., and Sato, Y. (2007) "Bond Stress-Slip Relationship between FRP Sheet and Concrete under Cyclic Load" Journal of Composites for Construction, ASCE, 11(4), 419-426.
18. Standards Australia (2003) "AS/NZS 4456.15: Masonry units, segmental pavers and flags – Methods of test. Method 15: Determining lateral modulus of rupture" ASI, Sydney, Australia.
19. Standards Australia. (2003) "AS3700-2001 Masonry Structures: Appendix D - Method of test for flexural strength" ASI, Sydney, Australia.
20. Park, R. (1989)"Evaluation of Ductility of Structures and Structural Assemblages from Laboratory Testing" Bulletin of the New Zealand Society for Earthquake Engineering, 3(22), 155-166.